

See discussions, stats, and author profiles for this publication at: <https://www.researchgate.net/publication/263940263>

Hierarchical Structures by Wetting Porous Templates with Electrospun Polymer Fibers

ARTICLE *in* ACS MACRO LETTERS · NOVEMBER 2011

Impact Factor: 5.76 · DOI: 10.1021/mz200008e

CITATIONS

23

READS

44

3 AUTHORS, INCLUDING:



Jiun-Tai Chen

National Chiao Tung University

58 PUBLICATIONS 1,076 CITATIONS

SEE PROFILE

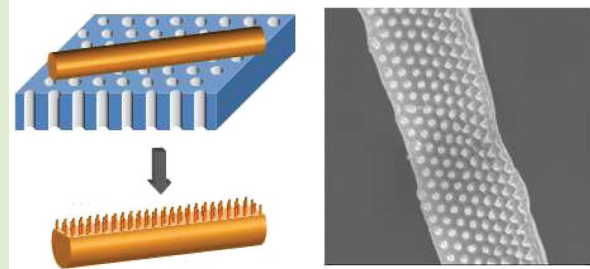
Hierarchical Structures by Wetting Porous Templates with Electrospun Polymer Fibers

Jiun-Tai Chen,* Wan-Ling Chen, and Ping-Wen Fan

Department of Applied Chemistry, National Chiao Tung University, Hsinchu, Taiwan 30050

 Supporting Information

ABSTRACT: We demonstrate a simple route to fabricate hierarchical structures by combining the electrospinning technique and the wetting of porous templates. Poly(methyl methacrylate) (PMMA) fibers are first prepared by electrospinning and are collected on a glass substrate. The PMMA fibers are then brought into contact with an anodic aluminum oxide template. Upon thermal annealing above the glass transition temperature of PMMA, wetting of the polymer chains into the nanopores occurs. After the removal of the AAO template, ordered arrays of nanorods on polymer fibers are obtained. This approach is also applied to polystyrene (PS), and similar structures are obtained. This work provides a promising approach to fabricate hierarchical polymer structures with sizes that can be controlled over the nanoscopic and microscopic length scales.



Hierarchical structures have attracted much attention recently because of their distinct properties and potential applications.^{1–4} Hierarchical structures with diverse functions are ubiquitous in nature.⁵ Wood and bone are typical examples of biological materials with hierarchical structures over many length scales.^{5–8} Their extraordinary mechanical properties are believed to be due to the rational adaptation of the structures at all levels of hierarchy.⁹ The topography of multiscale hierarchical structures also strongly affects the surface properties of biological materials.¹⁰ The surfaces of the lotus leaves, for example, consist of hierarchical structures in micro- and nanometer length scales and exhibit superhydrophobic properties and self-cleaning abilities.^{11,12} Because of these unique properties and potential applications, great efforts have been made to prepare hierarchical structures.^{13,14} Many biomimetic materials have been developed, and special properties such as superhydrophobicity are obtained by incorporating lotus-leaf-like or other bioinspired hierarchical structures.^{15,16} Although there have been many techniques to generate hierarchical structures, it remains a challenge to precisely control the structures in both the micrometer and nanometer range. Such control helps us to understand the structure–property relationship of hierarchical materials, enabling the rational design of novel materials for advanced devices and applications. Therefore, it is necessary to develop fabrication methods in which the structures can be independently and precisely controlled in different length scales.

Here, we report a simple method to prepare hierarchical polymer structures by combining the electrospinning technique and wetting of porous templates. The first length scale of ordering of these hierarchical structures is generated by the electrospinning process. Electrospinning is an efficient technique to prepare polymer fibers from polymer solutions,

with a diameter range from nanometers to a few micrometers.¹⁷ In the electrospinning process, a high potential difference is applied to create an electrically charged jet of polymer solution or melt, which dries or solidifies to produce polymer fibers. Electrospun polymer fibers have different applications such as sensors,¹⁸ filtration,¹⁹ drug delivery,²⁰ tissue engineering,^{21,22} catalysis,²³ and wound dressing.²⁴

In this study, the second length scale of ordering on the electrospun fibers is generated by wetting porous anodic aluminum oxide (AAO) templates. Template wetting has been widely used to prepare on-dimensional nanomaterials.^{25–27} The template is simply used as a scaffold, and the shapes of the nanomaterials is controlled by the geometry of the template. Different precursor materials, such as polymers, can be introduced into the nanopores of the templates by wetting or evaporation on the walls of the template.²⁵ The surface tension of the pore wall is usually high and the precursor materials wet the surface of the walls to reduce the surface energy. The template wetting method also enables the fabrication of nanomaterials made of multiple components.²⁷ The nanomaterials made by template wetting can be released by selectively removing the template. These nanomaterials have been demonstrated in different applications, such as photovoltaics,²⁸ photodetectors,²⁹ and biosensors.³⁰ Different materials have been used as templates for the generation of nanomaterials, but ion-track-etched membranes and anodic aluminum oxide (AAO) templates are the most commonly used templates.³¹ Ion-tracked membranes are usually prepared by polycarbonate

Received: August 7, 2011

Accepted: October 6, 2011

Published: November 9, 2011

or polyester films and are commercially available.³² But the porosity of the ion-tracked membranes is low and the nanochannels are usually randomly distributed.²⁵

The AAO templates that contain cylindrical pores are produced electrochemically from aluminum, and the sizes of the pores can be controlled by the anodization conditions.^{33,34} These templates have been widely used to prepare one-dimensional nanomaterials such as metallic and semiconductor nanowires,³⁵ carbon nanotubes,^{36,37} and polymer nanotubes.³⁸ The main advantage of using the AAO templates is their well-controlled pore sizes. In addition, the AAO templates can be easily removed after the preparation of the nanomaterials by using a selective etching solution such as a weak base or a weak acid. Using porous templates, free-standing polymer nanorods have been demonstrated to form on top of polymer films or even on top of polymer microspheres.³⁹ By bringing the electrospun polymer fibers into contact with the nanopores of the AAO templates followed by the wetting process, we are able to prepare hierarchical polymer structures with nanorods on top of the electrospun fibers.

Previously, electrospinning has been used to prepare hierarchical structures.^{40–43} For example, Hou and Reneker reported the preparation of carbon nanotubes on electrospun carbon fibers.⁴¹ The carbon fibers were generated by the carbonization of electrospun polyacrylonitrile fibers. Then the carbon nanotubes were formed by the catalysis of Fe nanoparticles embedded in the carbon fibers by exposing the fibers to hexane vapor.⁴¹ Ostermann et al. also synthesized single-crystal V₂O₅ nanorods grown on electrospun TiO₂ nanofibers by calcining composite nanofibers consisting of V₂O₅, TiO₂, and poly(vinylpyrrolidone).⁴² Although hierarchical structures were generated by various methods, most methods to fabricate hierarchical structures using electrospun fibers still fail to generate the second length scale of ordering in a controlled way. By comparison, here we prepare hierarchical polymer structures in which the sizes of the nanorods and the fibers can be well controlled.

An overview of our approach to prepare the hierarchical structure is presented in Figure 1. Polymer fibers are generated by electrospinning. At first, the polymers are dissolved in a suitable solvent such as DMF and are ejected from a capillary nozzle. Under the electric field, the polymer solution is drawn into a polymer jet at the end of the nozzle followed by a whipping process caused by electrostatic repulsion.⁴⁵ The nanometer- or micrometer-sized polymer fibers are deposited on the grounded collector after solvent evaporation. The fibers are then collected and are placed on top of an AAO template. Commercial AAO templates or synthesized AAO templates are both used in the study. The nanopores of the commercial AAO template are ~100–400 nm and are more irregular in shape. The synthesized AAO templates prepared by the second anodization method have more regular and well-packed nanopores.³⁴ The polymer fibers which are brought into contact with the AAO templates can wet the walls of the nanopores after thermal annealing. The polymer is drawn into the nanopores by capillary forces, forming nanorods whose length is governed by the time allowed for the polymer to be drawn into the nanopores. The hierarchical structures with nanorods on top of the polymer fibers can be obtained after removing the AAO templates selectively using an NaOH solution.

Electrospinning is a useful technique to make polymer fibers. If suitable solvents are available, almost all kinds of polymers

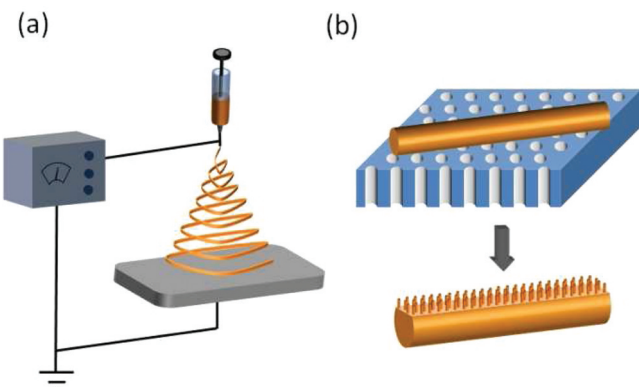


Figure 1. Schematic illustration of the approach to make hierarchical polymer structures based on electrospinning and wetting of porous templates. (a) The setup to prepare electrospun polymer fibers. A polymer solution is ejected from a capillary nozzle under the electric field, and electrospun polymer fibers are formed after drying of the solvent. (b) The electrospun polymer fibers are collected and are placed on top of the AAO templates. After thermal annealing above the glass transition temperatures of the polymers, wetting of the polymers occurs inside the walls of the nanopores of the AAO templates, resulting in nanorods on top of the electrospun polymer fibers. The hierarchical polymer structures can be released by removing the AAO templates using selective etching solution such as a weak base (NaOH).

can be made as fibers by the electrospinning method. The size and morphology of the electrospun polymer fibers are controlled by different experimental factors such as polymer molecular weight, solution concentration, solvent, flow rate, voltage, nozzle size, or working distance.⁴⁶ Figure 2 shows the SEM images of electrospun fibers under different conditions. The concentration of the polymer solution is one of the most common ways to control the size and morphology of the electrospun fibers. When the polymer concentration is lower than a critical value, the viscosity of the solution is not high enough to maintain a stable polymer jet. The polymer liquid jet might break into droplets caused by the Rayleigh instability, and polymer fibers are unable to be formed.⁴⁷ For low solution viscosity, beads-on-string structures are also observed caused by the entanglement of polymer chains and the contraction of the jet,⁴⁸ as shown in Figure 2a. When the viscosity of the solution is larger, both the size of the beads and the distance between beads increase.⁴⁸ If the polymer concentration is higher than a critical value, polymer fibers without beaded defects are formed. In general, the diameter of the electrospun polymer fiber increases with the concentration of the polymer solution. Figure 2a–c show the polymer fibers generated from different concentrations while keeping all other experimental factors constant. Poly(methyl methacrylate) (PMMA; M_w 49k) was dissolved in DMF at different concentrations (Figure 2a, 25 wt %; Figure 2b, 30 wt %; Figure 2c, 35 wt %) with the flow rate of 1 mL/h and working distance of 10 cm under the voltage of 15 kV. The diameters of the electrospun PMMA fibers increase from ~1 μm for 25 wt % to ~4 μm for 35 wt %. It has to be noted that the polymer solution might be difficult to be ejected from the nozzle when the concentration is too high because of the increased viscosity. In addition to the polymer concentration, the solution viscosity is also determined by the molecular weight and molecular weight distribution of the polymers.⁴⁹ It has been reported that the onset of uniform fiber formation in relatively broader molecular weight distribution

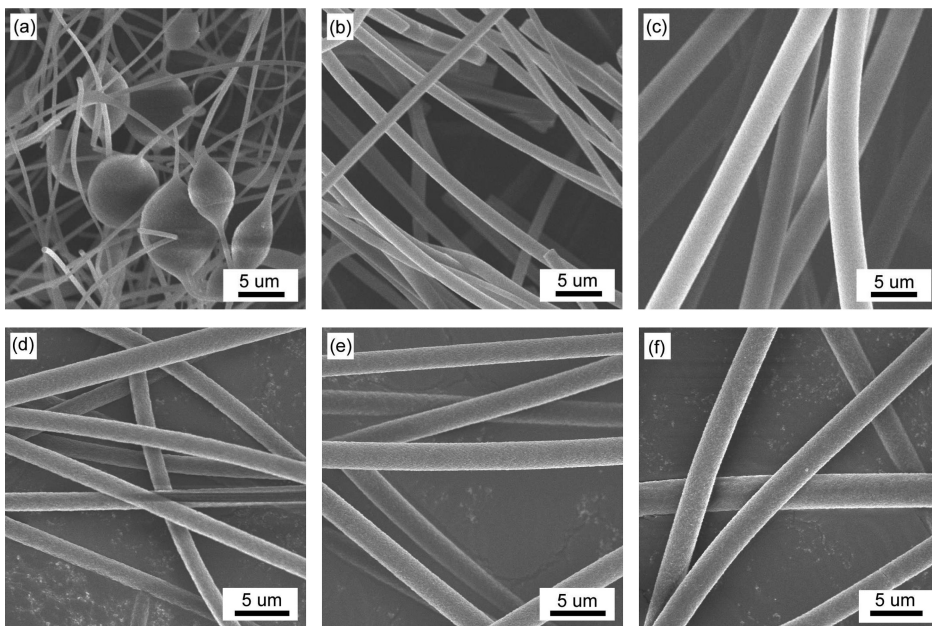


Figure 2. SEM images of electrospun PMMA fibers (M_w : 49k) under different electrospinning conditions: (a–c) voltage, 15 kV; flow rate, 1 mL/h; working distance, 10 cm; different polymer concentrations in DMF, (a) 25 wt %, (b) 30 wt %, (c) 35 wt %; (d–f) polymer concentration, 35 wt % in DMF; voltage, 10 kV; working distance, 10 cm; different flow rate, (d) 0.1 mL/h, (e) 0.5 mL/h, (f) 2.0 mL/h.

polymers occurs at a higher concentration comparing with that in the narrow molecular weight distribution polymers. The difference is because a relatively broad molecular distribution polymer has a wide distribution of the hydrodynamic radii and relaxation times of the chains in solution.⁴⁹

Another common way to control the diameters of the electrospun fibers is by varying the flow rate. The amount of the produced polymer fibers is proportional to the flow rate, and the diameter of the polymer fibers increases as the flow rate increases. Fridrikh et al. showed that varying the flow rate yields a $10^{2/3}$ -fold variation in the fiber diameter when the flow rate is over a certain range.⁵⁰ But if the flow rate is too fast, beaded fibers are formed. The fibers might also be partially dissolved by the residual solvent if the flow rate is too fast, and the morphology of the fiber can be affected. Figure 2d–f show the SEM images of electrospun fibers (49 k PMMA; 35 wt % in DMF; voltage, 10 kV; working distance, 15 cm) at different flow rates ((d) 0.1 mL/h; (e) 0.5 mL/h; (f) 2.0 mL/h). The average diameters of the fibers are larger when the flow rates are higher, and the relationship between the fiber diameters and the flow rate is plotted in the Supporting Information. The diameters and morphology of the electrospun fibers can also be controlled by other experimental conditions such as the applied voltage. When the applied voltage is higher, the electric field and the electrostatic force are stronger, resulting in the smaller diameters of the electrospun fibers.⁵¹

Anodic aluminum oxide (AAO) templates are used to control the second length scale of ordering on the electrospun polymer fibers. AAO templates are made by anodization of aluminum plates, and the pore density can be as high as 10^{11} pores/cm².⁵² In this study, we used two different kinds of AAO membranes as the templates, including the commercial AAO templates and the synthesized AAO templates. SEM images of the commercial and synthesized AAO templates are shown in Figure 3a and b, respectively. Figure 3a shows the SEM image of a commercial AAO template whose pore diameters are \sim 100–400 nm, and the pores are packed irregularly compared

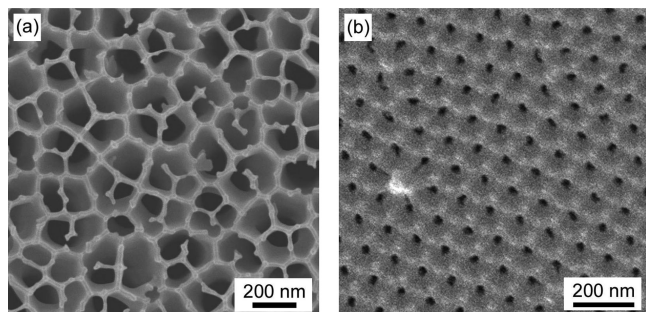


Figure 3. SEM images of the commercial and synthesized AAO templates: (a) A commercial AAO template with pore sizes \sim 100–400 nm; (b) A synthesized AAO template with pore sizes \sim 30–40 nm.

with those of the synthesized AAO templates. The pore sizes of the synthesized AAO templates shown in Figure 3b are more regular and are controlled by the anodization condition. Pore diameters ranging from 5 to 250 nm can be prepared by changing the type and the concentration of the electrolyte solution, the temperature, and the voltage of the anodization process.³⁴ The AAO template shown in Figure 3b was synthesized in 0.3 M oxalic acid at 40 V, and the pore size is \sim 30–40 nm with the pore-to-pore distance \sim 100 nm. The pore sizes can be increased by either increasing the voltage or by a pore-widening process using phosphoric acid (5 wt %) at 40 °C. The AAO templates can be easily removed by a selective etching solution. In this study, an NaOH solution was used to selectively remove the AAO templates without dissolving the polymer fibers.

After the electrospun polymer fibers are prepared, the polymer fibers are brought into contact with the AAO template by two different ways. The first way is to directly place the fibers on top of the AAO template. The second way is to collect the fibers on a substrate, and then place the AAO template on top of the fibers. Both ways are feasible, and it is critical to ensure good contact between the polymer fibers and the AAO

template for the wetting process to occur. The fibers can also be redispersed into nonsolvents such as ethylene glycol for good dispersion before being placed on top of the AAO template. The wetting process is critical in making the hierarchical structures, and there are two popular methods for wetting porous templates with polymers. The first method involves the wetting of porous templates using polymer solutions, and polymer nanotubes can be formed after the drying of solvents.⁵³ In the first method, annealing is not required because the solvent already provides enough mobility for the polymers to go into the nanopores. The second method to wet the nanopores is by heating a polymer film above the glass transition temperature or even the melting temperature for the wetting to occur.³⁸ Here, we use the second method of wetting by thermally annealing the sample above the glass transition temperature of the polymers (T_g of PMMA: 105 °C) for different periods of time. The rate of the polymer drawn into the nanopores of the templates can be estimated by the following equation:⁵⁴

$$\frac{dz}{dt} = R \gamma \cos \theta / (4\eta z) \quad (1)$$

where t is the time, z is the rod height, γ is the surface tension, θ is the contact angle, η is the viscosity, and R is the hydraulic radius (the ratio between the volume of the polymer in the pore and the area of solid/liquid interface). Therefore, the length of the polymer rods in the nanopores can be increased by using longer annealing time or lower polymer viscosity. The wetting behavior of polymer melts in cylindrical nanopores was also studied by Zhang et al. that the polymer can be formed as nanorods or nanotubes depending on whether the polymer is in the partial wetting state or in the complete wetting state.⁵⁵ The wetting transition from the partial wetting state to the complete wetting state depends on the molecular weight and molecular weight distribution of the polymers. For polymers with higher molecular weight, the temperature of wetting transition is also higher. The difference in the wetting rate between partial and complete wetting can be used to fractionate polymers with different molecular weights.⁵⁵

It has to be noted that there are only limited surfaces of the polymer fibers that are in contact with the nanopores of the AAO template before thermal annealing because of the cylindrical shape of the fibers. When the sample is heated above the glass transition temperature of the polymer, only polymers in these regions are initially drawn into the nanopores. At longer annealing time, larger surfaces of the polymer fibers are in contact with the template, and more polymers are drawn into the nanopores. Therefore, there is a distribution in the length of the nanorods on the polymer fibers. Ideally, the height of the nanorods near the center of the fiber should be higher than that of the nanorods near the edge of the fiber. Figure 4 shows the results of the SEM images of the electrospun PMMA fibers with nanorods. Figure 4a and b are from the fibers wetting with commercial AAO templates. The diameters of the electrospun polymer fibers are ~3–4 μm, and the pore sizes of the commercial AAO are ~100–400 nm. Some electrospun fibers are overlapping and melt together before or during the wetting process, as shown in Figure 4b. Figure 4c and d show the electrospun fibers wetting with the synthesized AAO templates. The diameters of the electrospun polymer fibers are ~600–800 nm, and the pore sizes of the synthesized AAO templates are ~30–40 nm. In Figure 4c, the meniscus shapes on the top of the polymer nanorods can be seen, which are the signatures of the capillary rising of the

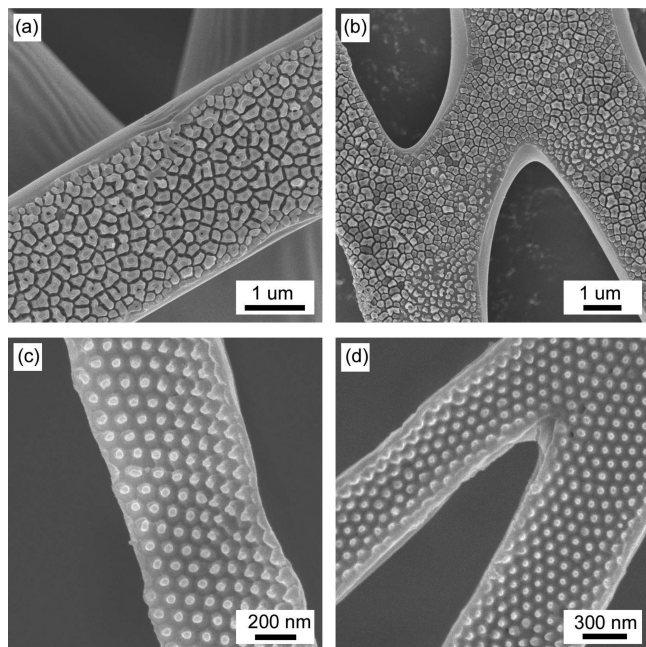


Figure 4. SEM images of electrospun PMMA fibers with nanorods. (a,b) Electrospun polymer fibers wetting into the nanopores of commercial AAO templates. The PMMA fibers were annealed at 150 °C for 30 min. The lengths of the nanorods are ~100 nm. (c,d) Electrospun polymer fibers wetting into the nanopores of synthesized AAO templates. The PMMA fibers were annealed at 135 °C for 10 min. The lengths of the nanorods are ~30–50 nm.

polymer melts into the nanopores. Fibers are also observed to overlap and melt together before or during the wetting process, as shown in Figure 4d. The fibers with nanorods shown in Figure 4c and d are from samples with short annealing time (135 °C for 10 min). The nanorods collapsed with longer annealing time, mainly caused by the high aspect ratio of nanorods and the capillary force driven by the removal of the etching solution, as shown in Figure 5.

To clarify the thermal annealing effect on the electrospun polymer fibers, we also annealed the fibers at 150 °C for 10 min without the presence of the AAO templates. The roughness of the fiber surfaces is decreased after the annealing process, as shown in Figure 6. The reduction of surface roughness is attributed to the decrease of surface energy at the polymer–air interface. Another possible outcome of the polymer fibers after thermal annealing is that the fibers may undergo surface undulation and break into spheres, the so-called Rayleigh-instability.⁵⁶ But this kind of instability was not observed in this work, which might be explained by the high viscosity and the strong polymer chain–chain interaction.

To demonstrate the universality of this work, we also study the fabrication of hierarchical structures by using polystyrene (PS), another commonly used polymer. As shown in Figure 7a, electrospun PS fibers are first obtained by electrospinning 20 wt % PS (M_w : 166k) in DMF under a voltage of 15 kV at a flow rate of 1 mL/h with a working distance of 15 cm. The diameters of the as-spun fibers are ~2–3 μm. After the PS fibers are brought into contact with a synthesized AAO template (pore diameters ~50 nm) followed by an annealing process at 135 °C for 15 min, hierarchical PS structures are obtained (see Figure 7b).

In conclusion, we develop a simple approach to fabricate hierarchical structures by placing electrospun polymer fibers in

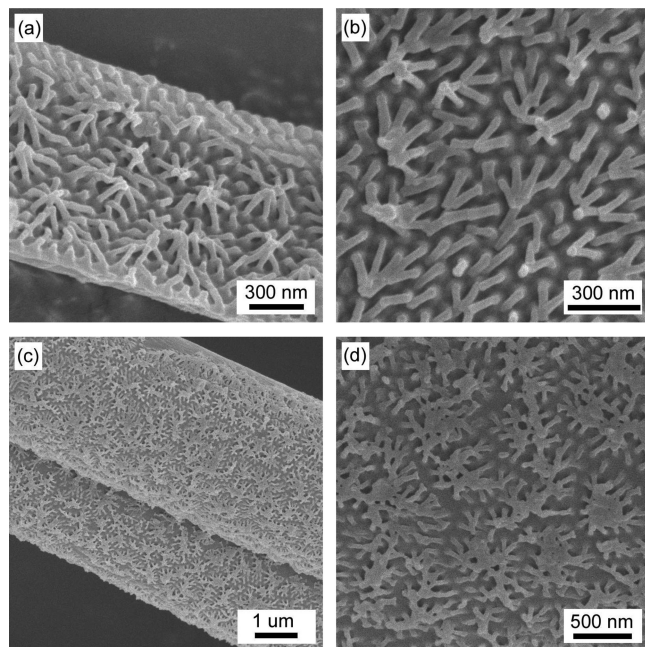


Figure 5. SEM images of electrospun PMMA fibers with collapsed nanorods. (a,b) Electrospun polymer fibers (fiber diameter $\sim 1 \mu\text{m}$) wetting into the nanopores of synthesized AAO templates (pore diameters $\sim 30\text{--}40 \text{ nm}$) at different magnifications. (c,d). Electrospun polymer fibers (fiber diameter $\sim 4 \mu\text{m}$) wetting into the nanopores of synthesized AAO templates (pore diameters $\sim 30\text{--}40 \text{ nm}$) at different magnifications.

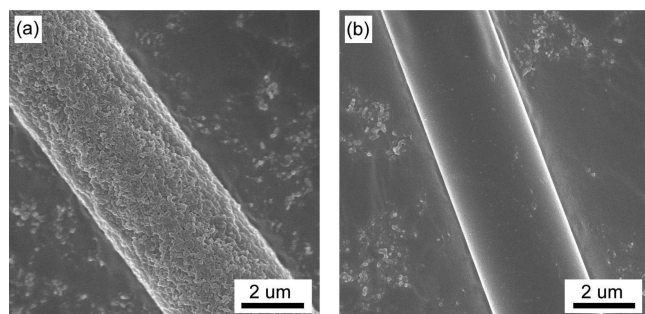


Figure 6. SEM images of electrospun polymer fibers before and after thermal annealing. The electrospun fibers were prepared from PMMA (M_w : 49k) and were annealed at 150 °C for 10 min.

contact with the nanopores of AAO templates. The advantage of this method is that the two size scales of ordering can be independently controlled. The first length scale is controlled by the diameters of the electrospun fibers, which can be varied by changing the electrospinning conditions such as the polymer concentration or the flow rate. The second length scale is controlled by the pore sizes of the AAO templates, which can be varied by changing the anodization conditions. For possible future work, we would like to apply this concept to other functional materials such as conjugated polymers and to study their electronic, mechanical, and surface properties for potential applications.⁵⁷

EXPERIMENTAL SECTION

Poly(methyl methacrylate) (PMMA; M_n , 26600; M_w , 49300; PDI, 1.85) and polystyrene (PS; M_n , 22900; M_w , 166500; PDI, 7.27) were purchased from Sigma Aldrich. *N,N*-Dimethylformamide (DMF) and tetrahydrofuran (THF) were obtained from TEDIA. Benzyltriethy-

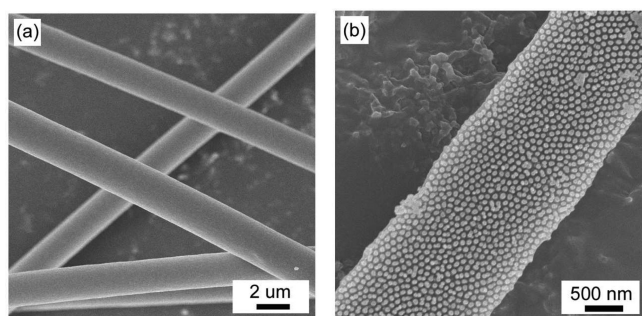


Figure 7. (a) SEM image of electrospun PS fibers. PS (M_w : 166k) fibers were obtained by electrospinning 20 wt % PS in DMF under a voltage of 15 kV at a flow rate of 1 mL/h with a working distance of 15 cm. The fiber diameters are $\sim 2\text{--}3 \mu\text{m}$. (b) SEM image of an electrospun PS fiber with nanorods. The electrospun PS fiber was wetted into the synthesized AAO templates (pore diameters $\sim 50 \text{ nm}$) at 135 °C for 15 min.

lammonium chloride (BTEAC) was purchased from Alfa Aesar. The commercial AAO membranes (pore diameter ca. 100–400 nm, thickness $\sim 60 \mu\text{m}$) were purchased from Whatman Ltd. The synthesized AAO templates were prepared according to the two-step anodization method developed by Masuda and co-workers.^{33,44} At first, a high-purity aluminum sheet (Sigma-Aldrich, 0.5 mm thick, 99.99%) was degreased in acetone and rinsed in an ethanol solution. Subsequently, the aluminum sheet was electropolished in a perchloric acid/ethanol mixture at 4 °C. The aluminum sheet was anodized at 40 V in 0.3 M oxalic acid at 17 °C for 12 h. After the resultant aluminum oxide film was chemically etched in a mixture of phosphochromic acid, a second anodization under the same conditions as for the first anodization was performed for different periods of time, depending on the required length of pores. The length of the pores is $\sim 4 \mu\text{m}$ when the second anodization is carried out for 2 h.

In a typical electrospinning experiment, 35 wt % PMMA (M_w , 49 kg/mol) solution in DMF was added into a syringe connected to a nozzle (inner diameter: 0.41 mm). The solution was fed at a constant rate (1 mL/h) through a syringe pump (KD Scientific). The nozzle was connected to a high-voltage power supply (SIMCO). The typical voltage range was 10–30 kV. The working distance range between the nozzle and the grounded collector was 10–20 cm. For some experiments, the organic salt BTEAC was also added to control the smoothness and the size of the electrospun fibers. After the electrospun fibers were brought into contact with the AAO templates, the samples were heated at 135 or 150 °C for different periods of time. The AAO templates were dissolved with 5 wt % NaOH_(aq) for 12 h, and the samples were repeatedly washed with water, followed by drying in vacuum. The microscopic features of the samples were investigated using a JEOL JSM-7401F scanning electron microscope (SEM) at an accelerating voltage of 10 kV. The samples were coated with 4 nm platinum before performing SEM measurements.

ASSOCIATED CONTENT

Supporting Information

The plot of the average diameter versus the flow rate of electrospun fibers and a SEM image of electrospun PMMA fibers with nanorods. This material is available free of charge via the Internet at <http://pubs.acs.org>.

AUTHOR INFORMATION

Corresponding Author

*E-mail: jtchen@mail.nctu.edu.tw.

Notes

The authors declare no competing financial interest.

ACKNOWLEDGMENTS

This work was supported by the National Science Council through Grant NSC 99-2218-E-009-028.

REFERENCES

- (1) Ikkala, O.; ten Brinke, G. *Chem. Commun.* **2004**, 2131–2137.
- (2) Nosonovsky, M.; Bhushan, B. *Mater. Sci. Eng., R* **2007**, 58, 162–193.
- (3) Lee, J. H. *Sens. Actuators, B* **2009**, 140, 319–336.
- (4) Innocenzi, P.; Malfatti, L.; Soler-Illia, G. *Chem. Mater.* **2011**, 23, 2501–2509.
- (5) Fratzl, P.; Weinkamer, R. *Prog. Mater. Sci.* **2007**, 52, 1263–1334.
- (6) Lichtenegger, H.; Muller, M.; Paris, O.; Riekel, C.; Fratzl, P. *J. Appl. Crystallogr.* **1999**, 32, 1127–1133.
- (7) Weiner, S.; Wagner, H. D. *Annu. Rev. Mater. Sci.* **1998**, 28, 271–298.
- (8) Rho, J. Y.; Kuhn-Spearing, L.; Ziopoulos, P. *Med. Eng. Phys.* **1998**, 20, 92–102.
- (9) Fratzl, P.; Gupta, H. S.; Paschalis, E. P.; Roschger, P. *J. Mater. Chem.* **2004**, 14, 2115–2123.
- (10) Koch, K.; Bhushan, B.; Barthlott, W. *Soft Matter* **2008**, 4, 1943–1963.
- (11) Jiang, L.; Zhao, Y.; Zhai, J. *Angew. Chem., Int. Ed.* **2004**, 43, 4338–4341.
- (12) Zorba, V.; Stratakis, E.; Barberoglou, M.; Spanakos, E.; Tzanetakis, P.; Anastasiadis, S. H.; Fotakis, C. *Adv. Mater.* **2008**, 20, 4049.
- (13) Soler-illia, G. J. D.; Sanchez, C.; Lebeau, B.; Patarin, J. *Chem. Rev.* **2002**, 102, 4093–4138.
- (14) Keizer, H. M.; Sijbesma, R. P. *Chem. Soc. Rev.* **2005**, 34, 226–234.
- (15) Patankar, N. A. *Langmuir* **2004**, 20, 8209–8213.
- (16) Gao, L. C.; McCarthy, T. J. *Langmuir* **2006**, 22, 5998–6000.
- (17) Huang, Z. M.; Zhang, Y. Z.; Kotaki, M.; Ramakrishna, S. *Compos. Sci. Technol.* **2003**, 63, 2223–2253.
- (18) Ding, B.; Wang, M. R.; Yu, J. Y.; Sun, G. *Sensors* **2009**, 9, 1609–1624.
- (19) Nisbet, D. R.; Rodda, A. E.; Finkelstein, D. I.; Horne, M. K.; Forsythe, J. S.; Shen, W. *Colloids Surf., B* **2009**, 71, CP1–12.
- (20) Li, W. J.; Mauck, R. L.; Tuan, R. S. *J. Biomed. Nanotechnol.* **2005**, 1, 259–275.
- (21) Pham, Q. P.; Sharma, U.; Mikos, A. G. *Tissue Eng.* **2006**, 12, 1197–1211.
- (22) Nair, L. S.; Bhattacharyya, S.; Laurencin, C. T. *Expert Opin. Biol. Ther.* **2004**, 4, 659–668.
- (23) Agarwal, S.; Wendorff, J. H.; Greiner, A. *Macromol. Rapid Commun.* **2010**, 31, 1317–1331.
- (24) Zahedi, P.; Rezaeian, I.; Ranaei-Siadat, S. O.; Jafari, S. H.; Supaphol, P. *Polym. Adv. Technol.* **2010**, 21, 77–95.
- (25) Martin, C. R. *Science* **1994**, 266, 1961–1966.
- (26) Steinhart, M.; Wendorff, J. H.; Greiner, A.; Wehrspohn, R. B.; Nielsch, K.; Schilling, J.; Choi, J.; Gosele, U. *Science* **2002**, 296, 1997–1997.
- (27) Steinhart, M.; Wehrspohn, R. B.; Gosele, U.; Wendorff, J. H. *Angew. Chem., Int. Ed.* **2004**, 43, 1334–1344.
- (28) Kim, J. S.; Park, Y.; Lee, D. Y.; Lee, J. H.; Park, J. H.; Kim, J. K.; Cho, K. *Adv. Funct. Mater.* **2010**, 20, 540–545.
- (29) O'Brien, G. A.; Quinn, A. J.; Tanner, D. A.; Redmond, G. *Adv. Mater.* **2006**, 18, 2379.
- (30) Kohli, P.; Wirtz, M.; Martin, C. R. *Electroanalysis* **2004**, 16, 9–18.
- (31) Huczko, A. *Appl. Phys. A: Mater. Sci. Process.* **2000**, 70, 365–376.
- (32) Apel, P. *Radiat. Meas.* **2001**, 34, 559–566.
- (33) Masuda, H.; Fukuda, K. *Science* **1995**, 268, 1466–1468.
- (34) Li, A. P.; Muller, F.; Birner, A.; Nielsch, K.; Gosele, U. *J. Appl. Phys.* **1998**, 84, 6023–6026.
- (35) Moon, J. M.; Wei, A. *J. Phys. Chem. B* **2005**, 109, 23336–23341.
- (36) Jeong, S. H.; Hwang, H. Y.; Lee, K. H.; Jeong, Y. *Appl. Phys. Lett.* **2001**, 78, 2052–2054.
- (37) Chen, J. T.; Shin, K.; Leiston-Belanger, J. M.; Zhang, M. F.; Russell, T. P. *Adv. Funct. Mater.* **2006**, 16, 1476–1480.
- (38) Steinhart, M., Supramolecular Organization of Polymeric Materials in Nanoporous Hard Templates. In *Self-Assembled Nanomaterials II: Nanotubes*; Springer-Verlag: Berlin, 2008; Vol. 220, pp 123–187.
- (39) Chen, J. T.; Chen, D.; Russell, T. P. *Langmuir* **2009**, 25, 4331–4335.
- (40) Yang, J. Y.; Zhan, S. H.; Wang, N.; Wang, X. M.; Li, Y.; Ma, W. Y.; Yu, H. B. *J. Dispersion Sci. Technol.* **2010**, 31, 760–769.
- (41) Hou, H. Q.; Reneker, D. H. *Adv. Mater.* **2004**, 16, 69.
- (42) Ostermann, R.; Li, D.; Yin, Y. D.; McCann, J. T.; Xia, Y. N. *Nano Lett.* **2006**, 6, 1297–1302.
- (43) Dai, Y. Q.; Lu, X. F.; McKiernan, M.; Lee, E. P.; Sun, Y. M.; Xia, Y. N. *J. Mater. Chem.* **2010**, 20, 3157–3162.
- (44) Masuda, H.; Satoh, M. *Jpn. J. Appl. Phys. Lett.* **1996**, 35, L126–L129.
- (45) Shin, Y. M.; Hohman, M. M.; Brenner, M. P.; Rutledge, G. C. *Polymer* **2001**, 42, 9955–9967.
- (46) Greiner, A.; Wendorff, J. H. *Angew. Chem., Int. Ed.* **2007**, 46, 5670–5703.
- (47) Hohman, M. M.; Shin, M.; Rutledge, G.; Brenner, M. P. *Phys. Fluids* **2001**, 13, 2201–2220.
- (48) Fong, H.; Chun, I.; Reneker, D. H. *Polymer* **1999**, 40, 4585–4592.
- (49) Gupta, P.; Elkins, C.; Long, T. E.; Wilkes, G. L. *Polymer* **2005**, 46, 4799–4810.
- (50) Fridrikh, S. V.; Yu, J. H.; Brenner, M. P.; Rutledge, G. C. *Phys. Rev. Lett.* **2003**, 90, 4.
- (51) Wang, C.; Hsu, C. H.; Lin, J. H. *Macromolecules* **2006**, 39, 7662–7672.
- (52) Almawlawi, D.; Coombs, N.; Moskovits, M. *J. Appl. Phys.* **1991**, 70, 4421–4425.
- (53) Cepak, V. M.; Martin, C. R. *Chem. Mater.* **1999**, 11, 1363–1367.
- (54) Kim, E.; Xia, Y. N.; Whitesides, G. M. *Nature* **1995**, 376, 581–584.
- (55) Zhang, M. F.; Dobriyal, P.; Chen, J. T.; Russell, T. P.; Olmo, J.; Merry, A. *Nano Lett.* **2006**, 6, 1075–1079.
- (56) Toimil-Molares, M. E.; Balogh, A. G.; Cornelius, T. W.; Neumann, R.; Trautmann, C. *Appl. Phys. Lett.* **2004**, 85, 5337–5339.
- (57) Tian, N.; Xu, Q. H. *Adv. Mater.* **2007**, 19, 1988.